Z. Kristallogr. **220** (2005) 884–894

Sound propagation in the time-domain by the Split-Operator technique

Diogenes Bosquetti and José Sánchez-Dehesa*

Valencia Nanophotonics Technology Center, Polytechnic University of Valencia, C/Camino de Vera s/n, 46022, Valencia, Spain

Received July 12, 2004; accepted January 5, 2005

Split-operator / Acoustics / Sound propagation / Scattering / Finite-difference-time-domain

Abstract. This work presents a finite-difference scheme to study the scattering of sound in the time-domain. It can be applied to heterogeneous fluids in any dimensionality. The scheme is based on the split-operator technique introduced in quantum mechanics to solve the time-dependent Schrödinger equation. This scheme presents advantages in comparison with the usual finite-difference time-domain algorithms. Its main characteristics are: a) its precision is of the order $(\Delta t)^3$; b) it can work with non-homogeneous space-discretizations; and c) it satisfies the energy conservation law. Here, the scheme is also applied to solve four simple tests cases in one-dimensional space.

Introduction

We address the problem of finding a numerical integration scheme for solving the second order differential equation that defines the sound propagation in inhomogeneous systems. The goal is to develop an efficient algorithm to study sound attenuation in a gas or fluid having periodic inclusions with different density and/or sound velocity. This problem is of current interest since is has been shown that, for example, structures consisting of rigid cylinders in air exhibit interesting properties regarding sound propagation [1–3]. Those structures were modeled by considering infinite periodic systems and by comparing the acoustic band structure with attenuation spectra measured in zero-order transmission experiments. Nevertheless, this method fails to describe features associated with actual finite structures. Thus, for example, attenuation bands (destructive interference) appear due to the existence of uncoupled bands at the air/periodic-structure interface. On the other hand, sound reinforcements (constructive interference) also appear in the spectra, which can be due to focusing effects produced by the borders of the structure [1, 3]. To overcome this difficulty the Transfer Matrix Method [4] has been recently introduced to solve the acoustic systems [5]. In this method the structures are infinite in the direction perpendicular to the sound propagation, and the main drawback is the huge numerical demand to get enough precision at high frequencies. Methods based on multiple scattering theory are a very good alternative when the sound scatterers have symmetric shape like cylinders or spheres [6–9]. The finite-difference time domain (FDTD) method introduced by Yee [10] has been extensively used to simulate the wave-propagation of electromagnetic waves in time-domain. In the same spirit the FDTD method has been employed to solve underwater acoustic problems [11]. Also, finite difference methods based on discretization of the second order wave equation have been developed in dealing with seismic wave propagation [12], and elastic wave propagation through periodic scatterers [13]. No limitations with respect to the shape of the scatterers exist in this method.

In this paper we introduce a new discretization scheme that deals with the differential equation for the sound propagation in non-homogeneous media. We have used a non-conventional set of canonical variables to define a phase-space where the Liouville theorem applies. Afterward, the corresponding first order differential equation associated with the spectral density is solved by the split-operator technique [14]. Finally, the operator of time evolution is employed to obtain the differential equation in space-domain which can be discretized in a non-uniform mesh. A preliminary version of this work has been published in a Conference Proceedings [15]. The paper is organized as follows. In Sect. II, the problem is formulated and solved by this new method. The solution found is valid for any arbitrary system in any dimensional space; i.e., one-dimensional (1D), two-dimensional (2D), and three-dimensional (3D). In Section III, we investigate some properties of the time step evolution matrix, obtained in the previous section. In Section IV, present numerical results when the method is applied to some 1D problems whose solutions are known. Finally, Sect. V summarize the work.

Theory and approach

Consider a linear inhomogeneous medium with space-dependent density $\varrho(\mathbf{r})$, and compressibility $\varkappa(\mathbf{r})$. The pres-

* Correspondence author (e-mail: jsdehesa@upvnet.upv.es)

sure field $\Phi(\mathbf{r},t)$ and particle velocity $\mathbf{v}(\mathbf{r},t)$ satisfy the following equations:

$$\frac{\partial \Phi(\mathbf{r},t)}{\partial t} = -\varkappa^{-1}(\mathbf{r})\,\overrightarrow{\nabla}\cdot\mathbf{v}(\mathbf{r},t)\,, \tag{1}$$

which is the equation of continuity, and

$$\varrho(\mathbf{r})\,\frac{\partial \mathbf{v}(\mathbf{r},t)}{\partial t} = -\overrightarrow{\nabla}\Phi(\mathbf{r},t)\,, \tag{2}$$

which is the Newton's law of motion. The compressibility is related to the sound velocity $c(\mathbf{r})$ through:

$$\varkappa(\mathbf{r}) = \frac{1}{\varrho(\mathbf{r})\,c^2(\mathbf{r})}\,. \tag{3}$$

These equations can be combined to obtain the well known second order partial differential equation for the scalar field:

$$\frac{\partial^2 \Phi(\mathbf{r},t)}{\partial t^2} = c^2(\mathbf{r})\,\varrho(\mathbf{r})\,\overrightarrow{\nabla}\cdot\left[\frac{1}{\varrho(r)}\,\overrightarrow{\nabla}\Phi(\mathbf{r},t)\right]. \tag{4}$$

At the same time, the system is considered non-dissipative, the energy is conserved, since its Hamiltonian is:

$$H = \tfrac{1}{2}\int \varrho(\mathbf{r})\,v^2(\mathbf{r},t)\,\mathrm{d}\mathbf{r} + \tfrac{1}{2}\int \varkappa(\mathbf{r})\,\Phi(\mathbf{r},t)\,\mathrm{d}\mathbf{r}\,. \tag{5}$$

We assume that $\varrho(\mathbf{r})$ and $c^2(\mathbf{r})$ are time independent, and, in composite media, their values change when going from one medium to the other. Also, they are correlated quantities since they are medium dependent.

Evaluating the divergence on the right side of Eq. (4), we can write:

$$\frac{\partial^2 \Phi(\mathbf{r},t)}{\partial t^2} = c^2(\mathbf{r})\,\{\nabla^2 - \overrightarrow{\nabla}(\ln[\varrho(\mathbf{r})])\cdot\overrightarrow{\nabla}\}\,\Phi(\mathbf{r},t)\,. \tag{6}$$

It is convenient to cast this second order differential equation in a pair of first order partial differential equations in time. For this, we define $\Lambda(\mathbf{r},t)$ to rewrite Eq. (6) as:

$$\frac{\partial \Phi(\mathbf{r},t)}{\partial t} = \Lambda(\mathbf{r},t)\,, \tag{7}$$

$$\frac{\partial \Lambda(\mathbf{r},t)}{\partial t} = \Gamma(\mathbf{r})\,\Phi(\mathbf{r},t) \tag{8}$$

where

$$\Gamma(\mathbf{r}) = c^2(\mathbf{r})\,\{\nabla^2 - \overrightarrow{\nabla}\ln[\varrho(\mathbf{r})]\cdot\overrightarrow{\nabla}\}\,. \tag{9}$$

The variables $\Phi(\mathbf{r},t)$ and $\Lambda(\mathbf{r},t)$ are canonical and define a multidimensional phase-space, where the phase density $\sigma(\Phi,\Lambda,t)$ [18], which verifies the Liouville theorem; *i.e.*, $\mathrm{d}\sigma(\Phi,\Lambda,t)/\mathrm{d}t = 0$. This density has an explicit time dependence plus an implicit time dependence in Φ and Λ. So, the total time derivative $\mathrm{d}\sigma(\Phi,\Lambda,t)/\mathrm{d}t$ is a sum of three different terms

$$\frac{\mathrm{d}\sigma(\Phi,\Lambda,t)}{\mathrm{d}t} = \frac{\partial\sigma}{\partial\Lambda}\,\frac{\partial\Lambda(\mathbf{r},t)}{\partial t} + \frac{\partial\sigma}{\partial\Phi}\,\frac{\partial\Phi(\mathbf{r},t)}{\partial t} + \frac{\partial\sigma}{\partial t}\,. \tag{10}$$

Making use of Eqs. (7)–(8) the Liouville equation is obtained:

$$\frac{\partial\sigma(\Phi,\Lambda,t)}{\partial t} = -\left[\Lambda(\mathbf{r},t)\,\frac{\partial}{\partial\Phi} + (\Gamma(\mathbf{r})\,\Phi(r,t))\,\frac{\partial}{\partial\Lambda}\right] \times \sigma(\Phi,\Lambda,t)\,. \tag{11}$$

To study the time evolution of the spectral density between some initial time t_i until a final time t_f it is convenient to define the corresponding time propagator operator $U(t_f,t_i)$. For this, we put Eq. (11) in an exponential form, by integrating from t_i to t_f:

$$\sigma(\Phi,\Lambda,t_f) = U(t_f,t_i)\,\sigma(\Phi,\Lambda,t_i)\,, \tag{12}$$

where

$$U(t_f,t_i) = \exp\left\{-\int_{t_i}^{t_f}\left[\Gamma(\mathbf{r})\,\Phi(\mathbf{r},t)\,\frac{\partial}{\partial\Lambda} + \Lambda(\mathbf{r},t)\,\frac{\partial}{\partial\Phi}\right]\mathrm{d}t\right\}. \tag{13}$$

Here a remark needs to be made. If the coefficients $\Gamma(\mathbf{r})\,\Phi(\mathbf{r},t)$ and $\Lambda(\mathbf{r},t)$ are time-independent, the time interval $[t_i,t_f]$ can be arbitrarily chosen. In any other case, the total interval can be divided in a number of M subintervals Δt_n, such that:

$$\begin{aligned}\exp&\left\{\int_{t_i}^{t_f}\Upsilon(\mathbf{r},t)\,\mathrm{d}t\right\}\\ &= \exp\left\{\int_{t_i}^{t_2}\Upsilon(\mathbf{r},t_1)\,\mathrm{d}t + \int_{t_2}^{t_3}\Upsilon(\mathbf{r},t_2)\,\mathrm{d}t\right.\\ &\qquad\left. + \ldots + \int_{t_{M-1}}^{t_f}\Upsilon(\mathbf{r},t_M)\,\mathrm{d}t\right\}\end{aligned} \tag{14}$$

where

$$\begin{aligned} &t_n \equiv t_i + \sum_{k=1}^{n-1}\Delta t_k\,; \qquad t_1 = t_i\,, \qquad t_M = t_f - \Delta t_M\,,\\ &\Upsilon(\mathbf{r},t_n) \equiv -\left[\Lambda(\mathbf{r},t_n)\,\frac{\partial}{\partial\Phi} + (\Gamma(\mathbf{r})\,\Phi(\mathbf{r},t_n))\,\frac{\partial}{\partial\Lambda}\right]. \end{aligned} \tag{15}$$

The time subintervals, $\Delta t_n = t_{n+1} - t_n$, must be small enough so that the time dependence on the parameters $\Gamma(\mathbf{r})\,\Phi(\mathbf{r},t)$ and $\Lambda(\mathbf{r},t)$ can be neglected, *i.e.*, $\Phi(\mathbf{r},t_n+\Delta t_n) \approx \Phi(\mathbf{r},t_n)$ and $\Lambda(r,t_n+\Delta t_n) \approx \Lambda(\mathbf{r},t_n)$. In this limit, the total time operator is:

$$\begin{aligned}U(t_f,t_i) = U&\left(t_f, t_i + \sum_{n=1}^{M-1}\Delta t_n\right)\\ &\times U\left(t_i + \sum_{n=1}^{M-1}\Delta t_n, t_i + \sum_{n=1}^{M-2}\Delta t_n\right)\\ &\times \ldots \times U(t_i + \Delta t_1, t_i)\,.\end{aligned} \tag{16}$$

It consists of successive applications of the M operators $U(\Delta t_n,t_n)$,

$$U(t_f,t_i) = \prod_{n=1}^{M}\left[U(\Delta t_n,t_n)\right] \tag{17}$$

where

$$U(\Delta t_n,t_n) = \exp\left\{-\Delta t_n\;\Upsilon(\mathbf{r},t_n)\right\}. \tag{18}$$

Therefore, the exponential form of the Liouville equation, Eq. (12), is

$$\sigma(\Phi,\Lambda,t_f)=\prod_{n=1}^{M} U(\Delta t\,,t_n))\,\sigma(\Phi,\Lambda,t_i)\,, \tag{19}$$

with

$$t_f-t_i=\sum_{n=1}^{M}\Delta t_n\,.$$

Time evolution of Φ, Λ: the Split-Operator technique

The M subintervals can be chosen equals with no lost of generality; i.e., $\Delta t_n=\Delta t$, $\forall n$. Let us study the time evolution of variables Φ and Λ between some initial time $t_n=t_i+(n-1)\,\Delta t$ up to a final time t_{n+1} separated by a step interval Δt, $t_{n+1}=t_n+\Delta t$, n being an integer in the interval $[1, M]$. As discussed before, Eq. (19) can be applied to this case:

$$\begin{aligned}&\sigma(\Phi,\Lambda,t_{n+1})\\&=\exp\left\{-\Delta t\left[\Lambda\,\frac{\partial}{\partial\Phi}+(\Gamma(\mathbf{r})\,\Phi(\mathbf{r},t_n))\,\frac{\partial}{\partial\Lambda}\right]\right\}\\&\quad\times\sigma(\Phi,\Lambda,t_n)\,.\end{aligned} \tag{20}$$

The differential operators $A_\Phi\equiv\Lambda(\mathbf{r},t_n)\,\dfrac{\partial}{\partial\Phi}$ and $B_\Lambda\equiv(\Gamma(\mathbf{r})\,\Phi(\mathbf{r},t_n))\,\dfrac{\partial}{\partial\Lambda}$ in the expression above do not commute and therefore, we cannot put the exponential as a product of two exponential; i.e.:

$$\exp\left[-\Delta t(A_\Phi+B_\Lambda)\right]\neq\exp\left(-\Delta t\,A_\Phi\right)\times\exp\left(-\Delta t\,B_\Lambda\right). \tag{21}$$

The relationship between the differential operators on both sides of inequality (21) is given by the Glauber's formula [16]. In Appendix A this formula is extended to the case of three different operators A, B and C to show that the special condition $A=C$, reduces the error of the approximation consisting of applying the single exponential operator in Eq. (20) as a sequential application of exponential operators containing only one single operator in the exponent. In other words, we can use the following approach:

$$\begin{aligned}&\exp\left[-\Delta t\left(\frac{A_\Phi}{2}+B_\Lambda+\frac{A_\Phi}{2}\right)\right]\\&\approx\exp\left(-\Delta t\,\frac{A_\Phi}{2}\right)\exp\left(-\Delta t\,B_\Lambda\right)\exp\left(-\Delta t\,\frac{A_\Phi}{2}\right)\\&\quad+O[(\Delta t^3)]\,.\end{aligned} \tag{22}$$

This approach represents the so called symmetrical split-operator (SSO) technique, which has been successfully applied in quantum mechanics to solve numerically the time dependent Schrödinger Eq. (14). Also, it has been proposed to solve physical problems in classical mechanics [17]. Thus, the splitting of an operator substantially reduces the error associated with applying it consecutively.

In our case, two different splitting schemes can be developed. The first one is:

$$\begin{aligned}\sigma(\Phi,\Lambda,t_{n+1})\simeq&\exp\left(-\frac{\Delta t}{2}\,\Gamma\Phi\,\frac{\partial}{\partial\Lambda}\right)\\&\times\exp\left(-\Delta t\,\Lambda\,\frac{\partial}{\partial\Phi}\right)\\&\times\exp\left(-\frac{\Delta t}{2}\,\Gamma\Phi\,\frac{\partial}{\partial\Lambda}\right)\times\sigma(\Phi,\Lambda,t_n)\,.\end{aligned} \tag{23}$$

The second possibility is:

$$\begin{aligned}\sigma(\Phi,\Lambda,t_{n+1})\simeq&\exp\left(-\frac{\Delta t}{2}\,\Lambda\,\frac{\partial}{\partial\Phi}\right)\\&\times\exp\left(-\Delta t\,\Gamma\Phi\,\frac{\partial}{\partial\Lambda}\right)\\&\times\exp\left(-\frac{\Delta t}{2}\,\Lambda\,\frac{\partial}{\partial\Phi}\right)\times\sigma(\Phi,\Lambda,t_n)\,.\end{aligned} \tag{24}$$

Both schemes are identical us to terms in $(\Delta t)^3$. First, let us analyze the splitting scheme defined by Eq. (23). It is known that the action of an exponential operator $\exp\left(\vartheta\dfrac{\partial}{\partial x}\right)$, where ϑ is a parameter, produces a shift of the variable by ϑ, namely

$$\exp\left[\vartheta\,\frac{\partial}{\partial x}\right]f(x)=f(x+\vartheta)\,. \tag{25}$$

Therefore, we have to apply sequentially this property the three exponential operators in Eq. (23). The application of the first operator gives:

$$\begin{aligned}\sigma(\Phi,\Lambda,t_{n+1})=&\exp\left(-\frac{\Delta t}{2}\,\Gamma\Phi\,\frac{\partial}{\partial\Lambda}\right)\\&\times\exp\left(-\Delta t\,\Lambda\,\frac{\partial}{\partial\Phi}\right)\\&\times\sigma\left(\Phi,\Lambda-\frac{\Delta t}{2}\,\Gamma\Phi,\,t_n\right).\end{aligned} \tag{26}$$

The result of the second operator is:

$$\begin{aligned}\sigma(\Phi,\Lambda,t_{n+1})=&\exp\left(-\frac{\Delta t}{2}\,\Phi\,\frac{\partial}{\partial\Lambda}\right)\\&\times\sigma\left(\Phi-\Delta t\,\Lambda,\,\Lambda-\frac{\Delta t}{2}\right.\\&\left.\times\,\Gamma(\Phi-\Delta t\,\Lambda),\,t_n\right).\end{aligned} \tag{27}$$

Finally, after the application of the third operator we obtain:

$$\begin{aligned}&\sigma(\Phi,\Lambda,t_{n+1})\\&=\sigma\left[\Phi-\Delta t\left(\Lambda-\frac{\Delta t}{2}\,\Gamma\Phi\right),\left(1+\frac{\Delta t^2}{2}\,\Gamma\right)\right.\\&\quad\left.\times\left(\Lambda-\frac{\Delta t}{2}\,\Gamma\Phi\right)-\frac{\Delta t}{2}\,\Gamma\Phi,\,t_n\right].\end{aligned} \tag{28}$$

From this expression the relationship between the quantities at the $n+1$ temporal step, $\Phi^{n+1}(\mathbf{r})$ and $\Lambda^{n+1}(\mathbf{r})$, with the corresponding ones at t_n, $\Lambda^n(\mathbf{r})$ and $\Phi^n(\mathbf{r})$, can be obtained. It is given by the following 2×2 matrix equation:

$$\begin{bmatrix} \Phi^{n+1}(\mathbf{r}) \\ \Lambda^{n+1}(\mathbf{r}) \end{bmatrix} = \mathbf{Y}(\mathbf{r},\Delta t) \times \begin{bmatrix} \Phi^{n}(\mathbf{r}) \\ \Lambda^{n}(\mathbf{r}) \end{bmatrix} \tag{29}$$

where

$$\mathbf{Y}(\mathbf{r},\Delta t) = \begin{bmatrix} \alpha_{11}(\mathbf{r},\Delta t) & \alpha_{12}(\mathbf{r},\Delta t) \\ \alpha_{21}(\mathbf{r},\Delta t) & \alpha_{22}(\mathbf{r},\Delta t) \end{bmatrix}, \tag{30}$$

and the coefficients $\alpha_{11},\ \alpha_{12},\ \alpha_{21},\ \alpha_{22}$ are:

$$\begin{aligned} \alpha_{11}(\mathbf{r},\Delta t) &= 1+\frac{\Delta t^2}{2}\,\Gamma(\mathbf{r})\,, \\ \alpha_{12}(\mathbf{r},\Delta t) &= -\Delta t\,, \\ \alpha_{21}(\mathbf{r},\Delta t) &= -\Delta t\,\Gamma(\mathbf{r})\left[1+\frac{\Delta t^2}{4}\,\Gamma(\mathbf{r})\right], \\ \alpha_{22}(\mathbf{r},\Delta t) &= 1+\frac{\Delta t^2}{2}\,\Gamma(\mathbf{r})\,. \end{aligned} \tag{31}$$

In similar form, the second temporal propagation scheme can be expressed by the very same Eq. (29), but with the following coefficients:

$$\begin{aligned} \alpha_{11}(\mathbf{r},\Delta t) &= 1+\frac{\Delta t^2}{2}\,\Gamma(\mathbf{r})\,, \\ \alpha_{12}(\mathbf{r},\Delta t) &= -\Delta t\left[1+\frac{\Delta t^2}{4}\,\Gamma(\mathbf{r})\right], \\ \alpha_{21}(\mathbf{r},\Delta t) &= -\Delta t\,\Gamma(\mathbf{r})\,, \\ \alpha_{22}(\mathbf{r},\Delta t) &= 1+\frac{\Delta t^2}{2}\,\Gamma(\mathbf{r})\,. \end{aligned} \tag{32}$$

Therefore, if we know the variables at some initial time t_i, their values at the final time t_f which is separated by M equal time steps Δt, are obtained by:

$$\begin{bmatrix} \Phi(\mathbf{r},t_f) \\ \Lambda(\mathbf{r},t_f) \end{bmatrix} = \begin{bmatrix} \alpha_{11}(\mathbf{r},\Delta t) & \alpha_{12}(\mathbf{r},\Delta t) \\ \alpha_{21}(\mathbf{r},\Delta t) & \alpha_{22}(\mathbf{r},\Delta t) \end{bmatrix}^M \begin{bmatrix} \Phi(\mathbf{r},t_i) \\ \Lambda(\mathbf{r},t_i) \end{bmatrix}. \tag{33}$$

The differential problem in the equations above is transformed into an algebraic problem by calculating the corresponding derivatives using finite-difference algorithms. In order to make such a calculation a discretization of the space has to be performed. Let us remark that the formulation introduced above is applicable to problems defined in any dimensions; 1D, 2D, and 3D. In the next section, we demonstrate the advantages of this new time-step evolution matrix (TSEM) algorithm in comparison with the standard Yee Algorithm. Afterward, in subsequent sections, the method will be applied to solve several 1D test cases.

Properties of the time step evolution matrix

In what follows we present some properties of the TSEM. With these properties in mind, the advantages of the SSO method in comparison with the standard FDTD become more evident. These properties are valid for the two distinct SSO algorithms. To treat both cases simultaneously, we add a new index, k, to distinguish the same quantity in the two algorithms ($k=1,\,2$).

We already know that the SSO algorithm produce two distinct TSEM. However, its Jacobian $J^{(k)}$ have the same value:

$$J^{(k)} = \begin{vmatrix} \alpha_{11}^{(k)}(\mathbf{r},\Delta t) & \alpha_{12}^{(k)}(\mathbf{r},\Delta t) \\ \alpha_{21}^{(k)}(\mathbf{r},\Delta t) & \alpha_{22}^{(k)}(\mathbf{r},\Delta t) \end{vmatrix} = 1\,. \tag{34}$$

This result reveals that the SSO preserves the initial system information, in each time step. Since $J^{(k)-1}=1$, we obtain the relationships:

$$\begin{aligned} \alpha_{11}^{(k)}(\mathbf{r},\Delta t) &= \frac{\partial \Phi^{j+1}}{\partial \Phi^{j}} = \frac{\partial \Lambda^{j}}{\partial \Lambda^{j+1}}\,, \\ \alpha_{12}^{(k)}(\mathbf{r},\Delta t) &= \frac{\partial \Phi^{j+1}}{\partial \Lambda^{j}} = -\frac{\partial \Phi^{j}}{\partial \Lambda^{j+1}}\,, \\ \alpha_{21}^{(k)}(\mathbf{r},\Delta t) &= \frac{\partial \Lambda^{j+1}}{\partial \Phi^{j}} = -\frac{\partial \Lambda^{j}}{\partial \Phi^{j+1}}\,, \\ \alpha_{22}^{(k)}(\mathbf{r},\Delta t) &= \frac{\partial \Lambda^{j+1}}{\partial \Lambda^{j}} = \frac{\partial \Phi^{j}}{\partial \Phi^{j+1}}\,. \end{aligned} \tag{35}$$

Another interesting property emerges, when we define the 2×2 matrices $\mathbf{I}$ and $\mathbf{R}^{(k)}$ respectively by

$$\mathbf{I} = \begin{bmatrix} 0 & 1 \\ -1 & 0 \end{bmatrix}, \tag{36}$$

and

$$\mathbf{R}^{(k)} = \mathbf{Y}^{t(k)} \times \mathbf{I} \times \mathbf{Y}^{(k)}\,, \tag{37}$$

where $\mathbf{Y}^{t(k)}$ is the TSEM transposed. Evaluating the matrix product $\mathbf{Y}^{t(k)} \times \mathbf{I} \times \mathbf{Y}^{(k)}$, we attain the elements $r_{ij}^{(k)}$, which are Poisson brackets between $\Phi^{j+1(k)}$, $\Lambda^{j+1(k)}$ and $\Phi^{j(k)}$, $\Lambda^{j(k)}$:

$$\begin{aligned} r_{11}^{(k)} &= \left[\Phi^{j(k)},\,\Phi^{j(k)}\right]_{(\Phi^{j+1(k)},\,\Phi^{j+1(k)})}\,, \\ r_{12}^{(k)} &= \left[\Phi^{j(k)},\,\Lambda^{j(k)}\right]_{(\Phi^{j+1(k)},\,\Lambda^{j+1(k)})}\,, \\ r_{21}^{(k)} &= \left[\Lambda^{j(k)},\,\Phi^{j(k)}\right]_{(\Phi^{j+1(k)},\,\Lambda^{j+1(k)})}\,, \\ r_{22}^{(k)} &= \left[\Lambda^{j(k)},\,\Lambda^{j(k)}\right]_{(\Lambda^{j+1(k)},\,\Lambda^{j+1(k)})} \end{aligned} \tag{38}$$

where

$$\begin{aligned} &\left[\Phi^{j(k)},\,\Lambda^{j(k)}\right]_{(\Phi^{j+1(k)},\,\Lambda^{j+1(k)})} \\ &= \frac{\partial \Phi^{j+1(k)}}{\partial \Phi^{j(k)}}\,\frac{\partial \Lambda^{j+1(k)}}{\partial \Lambda^{j(k)}} - \frac{\partial \Lambda^{j+1(k)}}{\partial \Phi^{j(k)}}\,\frac{\partial \Phi^{j+1(k)}}{\partial \Lambda^{j(k)}}\,. \end{aligned} \tag{39}$$

Since that

$$\mathbf{R}^{(k)} = \begin{bmatrix} r_{11}^{(k)} & r_{12}^{(k)} \\ r_{21}^{(k)} & r_{22}^{(k)} \end{bmatrix} = \mathbf{I}\,, \tag{40}$$

the $\mathbf{R}^{(k)}$ matrix is symplectic, and the SSO algorithm obeys the condition for canonical transformation of coordinates.

Other interesting TSEM property is the conservation of the area element $|\mathrm{d}A^{(k)}(\mathbf{r},\, t_{j+1})|$, defined by the vectorial product between Φ^{j+1} and Λ^{j+1}:

$$|\mathrm{d}A^{(k)}(\mathbf{r},\, t_{j+1})| = \begin{vmatrix} \Phi^{j(k)} & \Lambda^{j(k)} & (\Phi^{j(k)} \wedge \Lambda^{j(k)}) \\ \alpha_{11}^{(k)}(\mathbf{r},\Delta t) & \alpha_{12}^{(k)}(\mathbf{r},\Delta t) & 0 \\ \alpha_{21}^{(k)}(\mathbf{r},\Delta t) & \alpha_{22}^{(k)}(\mathbf{r},\Delta t) & 0 \end{vmatrix} . \tag{41}$$

Evaluating this determinant, we have $\left|\mathrm{d}A^{(k)}(\mathbf{r}, t_{j+1})\right| = \left|\mathrm{d}A^{(k)}(\mathbf{r}, t_j)\right|$. It follows that the total area is conserved in each time step. As we see in example A in the next section, all of these properties are not verified by the standard FDTD method.

Application: sound propagation in one dimension

The sonic band structure of a 1D fluids with periodic modulations of their density was studied by Dowling [19]. This section is focused to develop the numerical algorithm that allows to study the propagation of sound in 1D fluids having a general space-dependent density $\varrho(x)$.

Let us consider a pressure wave-packet with gaussian shape that at $t = 0$ is centered at x_c. The pressure Φ and its time derivative Λ have the following initial conditions:

$$\Phi^0(x) = 1 + \Omega \exp\left[-\zeta(x - x_c)^2\right], \tag{42}$$

$$\Lambda^0(x) = 0, \tag{43}$$

where Ω is the wave-packet amplitude and ζ defines its width.

The relationship in Eq. (29) will be used to study the propagation of this wave-packet. Any of the coefficients in Eqs. (31) or Eqs. (32) can be employed. Here, the ones in Eqs. (32) are chosen because they are numerically simpler. The 1D recursion formulas up to first degree in Δt for Eq. (29) are:

$$\Phi^{n+1}(x) = \left[1 + \frac{\Delta t^2}{2}\, \Gamma(x)\right] \Phi^n(x) - \Delta t\, \Lambda^n(x), \tag{44}$$

$$\Lambda^{n+1}(x) = \Lambda^n(x) - \frac{\Delta t}{2}\, \Gamma(x)\left[\Phi^n(x) + \Phi^{n+1}(x)\right]. \tag{45}$$

Also, we want to quantify the usual kinematic magnitudes of the particles in the sound wave-packet: the displacement $\xi^n(x)$, velocity $v^n(x)$ and the acceleration $a^n(x)$. The continuity equation and Newton's third law, Eqs. (1) and (2) respectively, relate those magnitudes with the pressure and its time derivative:

$$\frac{\mathrm{d}\Phi^n(x)}{\mathrm{d}x} + \varrho(x)\, a^n(x) = 0, \tag{46}$$

$$\Lambda^n(x) + \varkappa^{-1}(x)\, \frac{\mathrm{d}v^n(x)}{\mathrm{d}x} = 0. \tag{47}$$

While $a(x)$ is obtained directly from Eq. (46), $v(x)$ must be obtained at each x_i point by integration of eq. (47):

$$v^n(x_i) = v^n(x_{i-1}) - \int_{x_{i-1}}^{x_i} \varkappa(x)\, \Lambda^n(x)\, \mathrm{d}x. \tag{48}$$

Finally, since $v(x,t) = \partial\xi/\partial t$, the displacement $\xi^n(x_i)$ is

$$\xi^n(x_i) = \xi^{n-1}(x_i) + \int_{t_{i-1}}^{t_i} v(x_i, t)\, \mathrm{d}t. \tag{49}$$

Equations (46)–(49) have to be consistent with the initial conditions. Therefore, at $t = 0$,

$$v^0(x) = \xi^0(x) = 0. \tag{50}$$

Now, lets turn our attention to the Γ operator [Eq. (9], which has the following form in 1D:

$$\Gamma(x) = c^2(x) \left\{ \frac{\partial^2}{\partial x^2} - \left(\frac{\partial}{\partial x} \ln\left[\varrho(x)\right] \right) \frac{\partial}{\partial x} \right\}. \tag{51}$$

A finite difference expression of this operator can be obtained by using a non-uniform spatial discretization in order to treat cases in which abrupt discontinuities of density and velocity exist. In what follows we develop the finite difference formulas to calculate both $\partial/\partial x$ and $\partial^2/\partial x^2$.

The positive distances a_i, b_i, c_i and d_i, in the neighborhood of an arbitrary x_i point are

$$\begin{aligned} a_i &= x_{i+2} - x_i, & b_i &= x_{i+1} - x_i, \\ c_i &= x_i - x_{i-1}, & d_i &= x_i - x_{i-2}. \end{aligned} \tag{52}$$

To obtain the partial derivatives of any general function $\Xi(x)$ with an error proportional to $O[(\Delta x)^5]$ (Δx being the distance between two neighboring points), we expand $\Xi(x)$ in Taylor's series around some x_i point,

$$\begin{aligned} \Xi(x_i + a_i) &= \Xi(x_i) + \frac{\partial\Xi}{\partial x}(x_i)\, a_i + \frac{1}{2!}\frac{\partial^2\Xi}{\partial x^2}(x_i)\, a_i^2 \\ &\quad + \frac{1}{3!}\frac{\partial^3\Xi}{\partial x^3}(x_i)\, a_i^3 + \frac{1}{4!}\frac{\partial^4\Xi}{\partial x^4}(x_i)\, a_i^4 + \dots, \\ \Xi(x_i + b_i) &= \Xi(x_i) + \frac{\partial\Xi}{\partial x}(x_i)\, b_i + \frac{1}{2!}\frac{\partial^2\Xi}{\partial x^2}(x_i)\, b_i^2 \\ &\quad + \frac{1}{3!}\frac{\partial^3\Xi}{\partial x^3}(x_i)\, b_i^3 + \frac{1}{4!}\frac{\partial^4\Xi}{\partial x^4}(x_i)\, b_i^4 + \dots, \\ \Xi(x_i - c_i) &= \Xi(x_i) - \frac{\partial\Xi}{\partial x}(x_i)\, c_i + \frac{1}{2!}\frac{\partial^2\Xi}{\partial x^2}(x_i)\, c_i^2 \\ &\quad - \frac{1}{3!}\frac{\partial^3\Xi}{\partial x^3}(x_i)\, c_i^3 + \frac{1}{4!}\frac{\partial^4\Xi}{\partial x^4}(x_i)\, c_i^4 - \dots, \\ \Xi(x_i - d_i) &= \Xi(x_i) - \frac{\partial\Xi}{\partial x}(x_i)\, d_i + \frac{1}{2!}\frac{\partial^2\Xi}{\partial x^2}(x_i)\, d_i^2 \\ &\quad - \frac{1}{3!}\frac{\partial^3\Xi}{\partial x^3}(x_i)\, d_i^3 + \frac{1}{4!}\frac{\partial^4\Xi}{\partial x^4}(x_i)\, d_i^4 - \dots. \end{aligned} \tag{53}$$

The expressions above can be cast in the following formula for $\partial\Xi(x_i)/\partial x$:

$$\frac{\partial\Xi(x_i)}{\partial x} = A_i\Xi(x_{i+2}) + B_i\Xi(x_{i+1}) + C_i\Xi(x_{i-1}) + D_i\Xi(x_{i-2}) + E_i\Xi(x_i), \tag{54}$$

where

$$A_i = -\frac{b_i c_i d_i}{a_i(a_i - b_i)\,(a_i + c_i\,)(a_i + d_i)}\,,$$
$$B_i = -\frac{a_i c_i d_i}{b_i(b_i - a_i)\,(b_i + c_i\,)(b_i + d_i)}\,,$$
$$C_i = \frac{a_i b_i d_i}{c_i(c_i + a_i)\,(c_i + b_i\,)(c_i - d_i)}\,,$$
$$D_i = \frac{a_i b_i c_i}{d_i(d_i + a_i)\,(d_i + b_i\,)(d_i - c_i)}\,,$$
$$E_i = -(A_i + B_i + C_i + D_i)\,. \tag{55}$$

A similar procedure gives:

$$\frac{\partial^2 \Xi(x_i)}{\partial x^2} = AA_i \Xi(x_{i+2}) + BB_i \Xi(x_{i+1}) + CC_i \Xi(x_{i-1}) + DD_i \Xi(x_{i-2}) + EE_i \Xi(x_i)\,, \tag{56}$$

where

$$AA_i = -\frac{2[b_i c_i + d_i(b_i - c_i)]}{a_i(a_i - b_i)\,(a_i + c_i)\,(a_i + d_i)}\,,$$
$$BB_i = -\frac{2[d_i a_i + c_i(a_i - d_i)]}{b_i(b_i - a_i)\,(b_i + c_i)\,(b_i + d_i)}\,,$$
$$CC_i = -\frac{2[d_i a_i - b_i(a_i - d_i)]}{c_i(c_i + a_i)\,(c_i + b_i\,)(c_i - d_i)}\,,$$
$$DD_i = -\frac{2[b_i c_i - a_i(b_i - c_i)]}{d_i(d_i + a_i)\,(d_i + b_i)\,(d_i - c_i)}\,,$$
$$EE_i = -(AA_i + BB_i + CC_i + DD_i)\,. \tag{57}$$

Notice that coefficients AA_i, BB_i, CC_i, DD_i and EE_i are proportional, respectively, to A_i, B_i, C_i, D_i and E_i. So, the coefficients of the second order derivative can be put in terms of the corresponding first derivatives.

The application of Γ gives:

$$\Gamma(x_i)\,\Xi(x_i) = \Gamma_{Ai}\Xi(x_{i+2}) + \Gamma_{Bi}\Xi(x_{i+1}) + \Gamma_{Ci}\Xi(x_{i-1}) + \Gamma_{Di}\Xi(x_{i-2}) + \Gamma_{Ei}\Xi(x_i) + O[(\Delta x)^5]\,, \tag{58}$$

where

$$\Gamma_{Ai} = c^2(x_i)\left\{\frac{2}{c_i} - \frac{2}{b_i} + \frac{2}{d_i} - \frac{\partial}{\partial x}\,(\ln[\varrho(x_i)])\right\} A_i\,,$$
$$\Gamma_{Bi} = c^2(x_i)\left\{\frac{2}{c_i} - \frac{2}{a_i} + \frac{2}{d_i} - \frac{\partial}{\partial x}\,(\ln[\varrho(x_i)])\right\} B_i\,,$$
$$\Gamma_{Ci} = c^2(x_i)\left\{\frac{2}{d_i} - \frac{2}{b_i} - \frac{2}{a_i} - \frac{\partial}{\partial x}\,(\ln[\varrho(x_i)])\right\} C_i\,,$$
$$\Gamma_{Di} = c^2(x_i)\left\{\frac{2}{c_i} - \frac{2}{b_i} - \frac{2}{a_i} - \frac{\partial}{\partial x}\,(\ln[\varrho(x_i)])\right\} D_i\,,$$
$$\Gamma_{Ei} = c^2(x_i)\left\{\frac{2}{d_i} + \frac{2}{c_i} - \frac{2}{a_i} - \frac{2}{b_i} - \frac{\partial}{\partial x}\,(\ln[\varrho(\mathbf{x}_i)])\right\} E_i\,, - 2c^2(\mathbf{x}_i)\left\{\frac{DD_i}{d_i} + \frac{CC_i}{c_i} - \frac{AA_i}{a_i} - \frac{BB_i}{b_i}\right\}. \tag{59}$$

Equations (59) define the finite difference scheme for $\Gamma(x)$. It will be applied in the following subsections to analyse the sound propagation in several 1D problems. The good performance of the method were demonstrated previously in 1D systems consisting of media with impedance mistmach [15]; the numerical results were in fairly good agreement with the analytical solutions. In what follows uniform and non-uniform systems having impedance matching will be analysed for the sake of completitude.

Test case 1: Sound propagation in a uniform medium: comparison with the standard FDTD method

The FDTD method introduced by Yee [10] to study the propagation of electromagnetic waves in isotropic media is conceptually simple and straightforward. In acoustics it requires the time discretization of Eqs. (1) and (2) by using a constant time step Δt:

$$\frac{\partial \Phi(x,t)}{\partial t} = \frac{\Phi^{n+1}(x) - \Phi^n(x)}{\Delta t} + O(\Delta t^2)\,, \tag{60}$$
$$\frac{\partial v(x,t)}{\partial t} = \frac{v^{n+1}(x) - v^n(x)}{\Delta t} + O(\Delta t^2)\,. \tag{61}$$

Then, Eqs. (1)–(2) can be reduced to the following matrix form:

$$\begin{pmatrix} \Phi^{n+1}(x) \\ v^{n+1}(x) \end{pmatrix} = \begin{pmatrix} \beta_{11}(x,t) & \beta_{12}(x,t) \\ \beta_{21}(x,t) & \beta_{22}(x,t) \end{pmatrix} \begin{pmatrix} \Phi^n(x) \\ v^n(x) \end{pmatrix}, \tag{62}$$

where

$$\beta_{11}(x,t) = \beta_{22}(x,t) = 1\,,$$
$$\beta_{12}(x,t) = -\Delta t\,\varkappa^{-1}(x)\,\partial/\partial x\,,$$
$$\beta_{21}(x,t) = -\Delta t\,\varrho^{-1}(x)\,\partial/\partial x\,. \tag{63}$$

Equation (62) defines the time step evolution matrix in the so called standard FDTD method, which is simpler than the equivalents based on the SSO technique [Eqs. (29)–(33)]. However, its simplicity pays a price: the Jacobian of the 2×2 matrix in Eq. (62) is not unitary; it contains non-zero terms in Δt^2 order. This non-unicity results in a progressive error in each time step, and consequently loss of initial system information. Also, since the method is restricted to very small $\Delta t/\Delta x$ ratios, it is extremely difficult to apply it in long time evolutions. The pressure time derivative $\Lambda(x,t)$ is obtained in this scheme by using the continuity condition, Eq. (2):

$$\Lambda^n(x) = -\varkappa^{-1}(x)\,\frac{\partial v^n(x)}{\partial x}\,. \tag{64}$$

Figures 1 and 2 show the comparison between the standard FDTD and the one based on the SSO technique, in the case of sound propagation in a uniform medium ($\varrho(x) = 1$; $c(x) = 1$) with no external perturbations. The units of mass, length and time along the rest of the article are gramme (g), centimeter (cm) and second (s), respectively. At $t = 0$ the gaussian wave-packet

$$\Phi^0(x) = 1 + 0.0013\exp\left[-0.001x^2\right],$$
$$\Lambda^0(x) = 0\,,$$

is created and travels freely along the x-axis. These are the initial conditions in time-evolution, which is calculated in

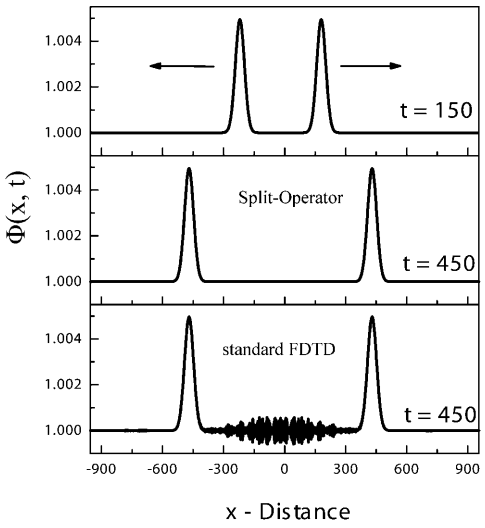

Fig. 1. Propagation of a sound wave packet with gaussian shape in a homogeneous medium. Time evolution of the sound pressure $\Phi(x,t)$. Comparison at $t = 450$ of the wave packets obtained with the standard FDTD method and the Split-Operator method.

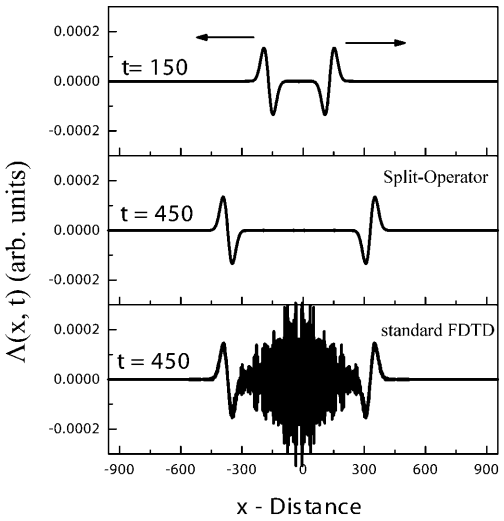

Fig. 2. Propagation of a sound wave packet with gaussian shape in a homogeneous medium. Time evolution of the sound pressure $\Lambda(x,t)$. Comparison at $t = 450$ of the wave packets obtained with the standard FDTD method and the Split-Operator method.

these two different algorithms. A non-uniform spatial discretization is employed, the parameters are described in Table 1. A constant time-step $\Delta t = 5 \times 10^{-4}$ is considered. The same space steps and time steps were employed in both algorithms.

Table 1. Discretization parameters employed in the simulations presented in Fig. 1. The parameters in the negative axis are the same.

D	Δx	n^0 of points	$\Delta t/\Delta x$
0–500	0.5	1000	10×10^{-4}
500–550	1.0	50	5×10^{-4}
550–625	1.5	50	3.33×10^{-4}
625–725	2.0	50	2.5×10^{-4}
725–800	2.5	30	2×10^{-4}
800–890	3.0	30	1.67×10^{-4}
890–995	3.5	30	1.43×10^{-4}

Once the initial wave-packet is free at $t = 0$, it splits in two equally wave-packets, each moving in opposite directions. While the wave-packet travels, numerical errors appear and grow in every time-step. At $t = 150$, Figs. 1–2 show that the errors are negligible in both algorithms. At $t = 450$, however, Fig. 1 shows some noise appearing in between the two packets for the FDTD algorithm. A similar conclusion can be drawn from results in Fig. 2, which shows the evolution of $\Lambda^n(x)$. Now the noise observed in the FDTD method start at earlier times. The order of the noise being comparable to the wave-packet height at $t = 450$. Let us remark that the result obtained with the FDTD method can be substantially improved by using "properly chosen" space and time steps.

Test case 2: Sound propagation in a layered system

Let us consider a layered system composed by three different homogeneous media, with distinct mass densities $\varrho_i (i = 1, 3)$, and sound velocities c_i. The values of these magnitudes and their corresponding acoustic impedances, $Z_i = \varrho_i c_i$, are listed in Table 1. Also, we consider that medium 2 is finite, with length $L = 400$, and is placed in between media 1 and 3, both considered semi-infinite (see Fig. 1). The transmission (T) and reflection (R) coefficients at one interface only depend of the impedance ratio of the media involved, $Z_{\text{incident}}/Z_{\text{transmitted}}$, and they are well known [20]:

$$T_{2\to1} = \frac{2}{Z_2/Z_1 + 1} = \frac{2}{3}\,; \qquad T_{2\to3} = \frac{2}{Z_2/Z_3 + 1} = \frac{4}{3}\,,$$

$$R_{2\to1} = \frac{Z_2/Z_1 - 1}{Z_2/Z_1 + 1} = \frac{1}{3}\,; \qquad R_{2\to3} = \frac{Z_2/Z_3 - 1}{Z_2/Z_3 + 1} = -\frac{1}{3}\,.$$

In both cases, the condition $T + R = 1$ is verified, but the negative sign of R indicates that $T > 1$.

In the system described we have studied the propagation in time domain of a gaussian wave-packet which is put at the middle of medium 2 in $t = 0$ and it is subjected to the initial condition $\Lambda^0(x) = 0$. The corresponding Eq. (33) has been solved by using a non-uniform mesh in the x-axis; more points were defined in the regions close to the interfaces. The pressure pattern as a function of time is shown in Fig. 3. At $t = 100$, it can be observed how the initial wave-packet is now divided in two equal packets traveling in opposites directions. After some time interval, $t = 250$, both wave-packets have crossed on the two interfaces and have been partially reflected. However, since the acoustics impedances are such that $Z_1 < Z_2 < Z_3$, two different phenomena occurs. At the $2 \to 1$ interface ($Z_2/Z_1 = 2$), the left wave-packet pass to a medium with a lower acoustic impedance. In this case, a phase inversion takes place on the reflected part, while the transmitted part has a peak lower than the incident. On the other hand, at the $2 \to 3$ interface ($Z_2/Z_3 = {}^1/_2$), the right wave-packet pass to a higher acoustic impedance media. Now, we have the opposite case; no phase inversion occurs on the reflected part, and the transmitted part has a peak greater than the incident. The theoretical predictions agree with the qualitative behavior observed in Fig. 3. Moreover, regarding quantitative results, in Table 2 we

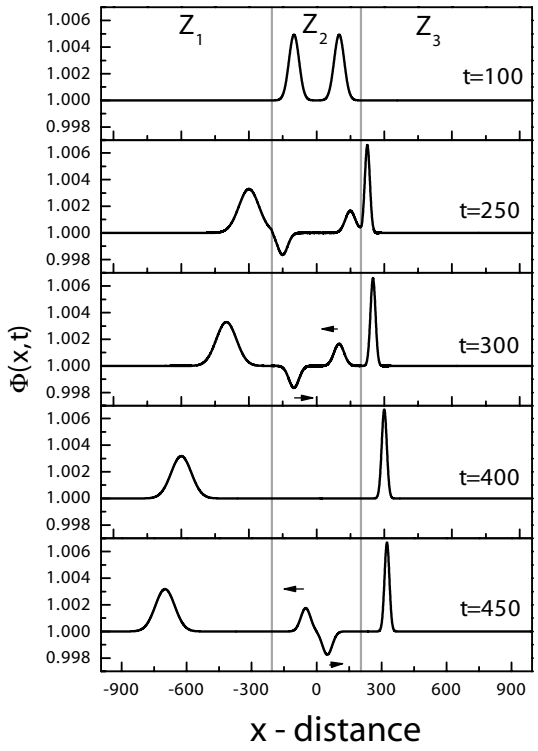

Fig. 3. Propagation of a sound wave packet in a layered acoustic structure. At $t = 0$, a gaussian wave packet is left at position $x = 0$. Afterward, it splits and move freely along the two possible paths in the one-directional space. At $t = 100$, the total wave packet will incides in the interfaces of this system. However, when this incidence occurs, different phenomenas will occur because the acoustics impedance $Z_1 < Z_2 < Z_3$. Since that $Z_2/Z_1 = Z_3/Z_2 = 2$, we have no phase inversion of reflected part of wave packet in $2 \rightarrow 1$ interface and the transmitted part the wave packet has a peak greater than the incident one. At the same time, for $2 \rightarrow 3$ interface, we have an phase inversion of transmitted wave packet, and the transmitted part is lower than the incident. In $t = 250$, we can see the transmission and reflected parts in the system. At $t = 400$, a total destructive interference occurs in medium 2. It happens because the reflection part of these two media is exactly the same. Finally, at $t = 450$, the second transmitted and reflected wave packets appears on the system.

show the comparison between different coefficients resulting from the SSOP technique and the ones analytically obtained.

Since the media are homogeneous, their group and phase velocities are equal inside a given medium. This

Table 2. Densities, sound velocities and acoustic impedances of the three homogeneous media in the layered structure under study.

	ϱ (g/cm)	c (cm/s)	Z (g/s)
medium 1	0.25	2.0	0.5
medium 2	1.0	1.0	1.0
medium 3	4.0	0.5	2.0

Table 3. Transmission and reflection coefficients.

Coeff.	SSO	Exact
$T_{2\rightarrow 1}$	0.646	0.667
$T_{2\rightarrow 3}$	1.354	1.333
$R_{2\rightarrow 1}$	0.354	0.333
$R_{2\rightarrow 3}$	0.354	0.333

Table 4. Values of densities, particle velocity and acoustic impedance in the media.

$t(s)$	$\langle x_R(t)\rangle_{2\rightarrow 1}$	$\langle x_T(t)\rangle_{2\rightarrow 1}$	$\langle x_R(t)\rangle_{2\rightarrow 3}$	$\langle x_T(t)\rangle_{2\rightarrow 3}$
250	1260	1100	1560	1610
350	1360	900	1460	1660
400	1410	800	1410	1685
500	1510	600	1310	1735

fact also can be check out in our algorithm. Let us define the average position of the reflected wave packet by $\langle x_R(t)\rangle$ and its analogue for the transmitted one by $\langle x_T(t)\rangle$. Table 3 shows their values at several times. From Table 3 the group velocity of reflected and transmitted wave packets at the $2 \rightarrow 1$ interface can be obtained:

$$v_{gR}(2 \rightarrow 1) = \frac{\langle x_R(t_2)\rangle_{2\rightarrow 1} - \langle x_R(t_1)\rangle_{2\rightarrow 1}}{t_2 - t_1} = 1.0 = c_2\,,$$

$$v_{gT}(2 \rightarrow 1) = \frac{\langle x_T(t_2)\rangle_{2\rightarrow 1} - \langle x_T(t_1)\rangle_{2\rightarrow 1}}{t_2 - t_1} = 0.5 = c_1\,.$$

Using an analogous procedure for the $2 \rightarrow 3$ interface, we also find that $v_{gR}(2 \rightarrow 3) = 1.0 = c_2$, and $v_{gT}(2 \rightarrow 3) = 0.5 = c_3$.

With regards to acoustic energy conservation, the method also verify such property with maximum accuracy.

Test case 3: Sound propagation across an acoustic medium with smooth variations of mass density and sound velocity

Let us consider an inhomogeneous medium of length $L = 500$ sandwiched between two semi-infinite uniform media with mass density, $\varrho_0 = 1$, and sound velocity, $c_0 = 1$. Also, it will be assumed that the medium has a density and velocity that change in such a way that its acoustical impedance matches the one of the surrounding media. In other words, $\varrho(x) = c^{-1}(x)$ and $Z(x) = \varrho(x)\,c(x) = 1$. The position dependence of $c(x)$ is modeled by a Lorentzian shape:

$$c(x) = \frac{c_{\max}}{1 + \varsigma(x - x_m)^2}\,, \qquad x_m - L/2 \leq x \leq x_m + L/2 \tag{65}$$

where the parameters are: $c_{\max} = 8$, $\varsigma = 5 \times 10^{-5}$, and $x_m = 375$.

If a sound wave packet impinges the medium on one side, it is expected that the packet shape will be distorted inside the inhomogeneous medium. Nevertheless, its initial shape will be recovered after crossing it. This result is a consequence of the impedance matching along the traveling distance. In other words, the total transmitted and the total reflected waves are one and zero, respectively, at every time step.

Figures 5 and 6 show, respectively, the time evolution of Φ and Λ for the case of a gaussian wave packet propagating through a barrier of length $L = 500$. In this simulation, a uniform spatial discretization has been used between two consecutive points, $\Delta x = 0.5$. A constant time-step $\Delta t = 5 \times 10^{-4}$ is employed. After $t = 0$, the initial wave packet (not shown) splits and one part travels along

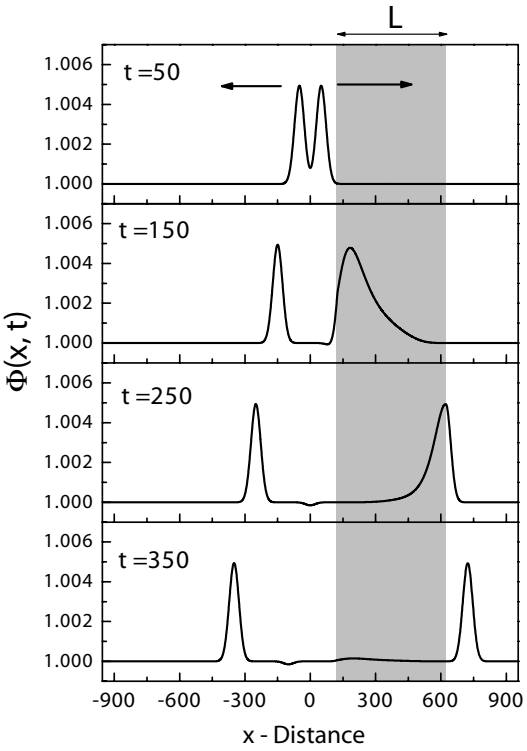

Fig. 4. Propagation of a sound wave packet with gaussian shape placed in front of an inhomogeneous medium (shadowed region of length L) having a constant specific acoustic impedance, but with a smooth variation of density and sound velocity [see Eq. (65)]. The initial wave packet is put at $x_c = 0$ and starts moving at $t = 0$ (not shown here). Behavior of the pressure $\Phi(x,t)$ at different time steps.

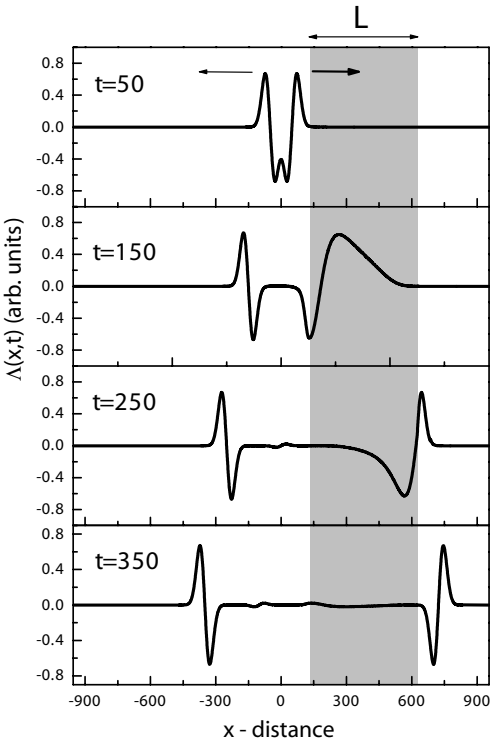

Fig. 5. Propagation of a sound wave packet with gaussian shape placed in front of an inhomogeneous medium (shadowed region of length L) having a constant specific acoustic impedance, but with a smooth variation of density and sound velocity [see Eq. (65)]. The initial wave packet is put at $x_c = 0$ and starts moving at $t = 0$ (not shown here). Behavior of the pressure derivative $\Lambda(x,t)$ at different time steps.

the positive x-direction, while the other one goes in the opposite direction. At $t = 50$, the front of the right packet impinges the barrier's left side. At subsequent times (see the plots at $t = 150$ and $t = 250$), a distortion in the packet is produced inside the barrier. The distortion gradually disappears and, finally, at $t = 350$, when the packet has completely passed the barrier, its shape equals the initial packet, coinciding with the one moving in the negative x-direction. Numerically, the peak heights of the packets are equal up to six digits.

Test case 4: Sound propagation across an acoustic superlattice with a perfect matching of impedances

Consider a homogeneous medium with constant density $\varrho_0 = 1$ and sound velocity $c_0 = 1$. In this system, a superlattice with ten periods is created in which the barriers have different values of density ($\varrho_1 = 2$) and velocity ($c_1 = 0.5$), but the same specific acoustic impedance $Z_1 = Z_0 = 1$. All barriers have length L and the separation between consecutive barriers is d. Therefore, the interface points are

$$\begin{cases} x_{2n} = x_0 + n(L+d) \\ x_{2n+1} = x_0 + n(L+d) + L \end{cases}, \tag{66}$$

where x_0 is the superlattice initial point and n are integers $n = 0, 1, 2, \ldots N$.

The perfect matching of specific acoustical impedances in the superlattice makes it transparent to sound propagation. Then it is expected that every wave-packet impinging on one side of the superlattice will be completely transmitted on the opposite side without reflections.

Figures 6 and 7 show the numerical simulation obtained by using an uniform space step ($\Delta x = 0.5$) and a constant time step ($\Delta t = 5 \times 10^{-4}$) for a superlattice with

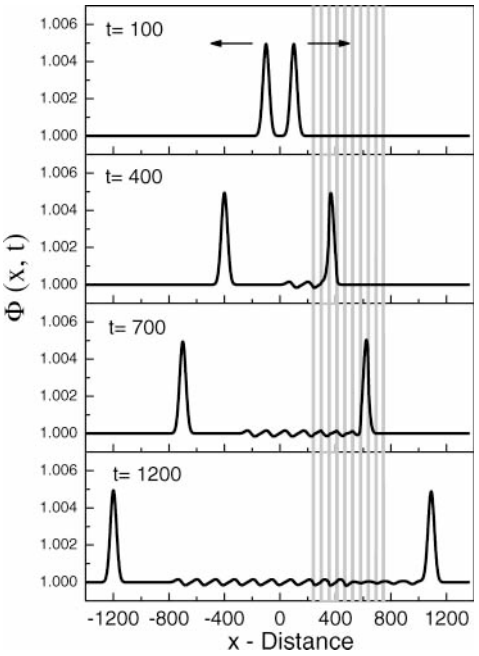

Fig. 6. Time evolution of a gaussian wavepacket put in front of an acoustic superlattice with ten periods. The sound pressure $\Phi(x,t)$ is shown at different time steps. All the layers have the same acoustic impedance as the surrounding media. The initial wavepacket (not shown here) is put at $x_c = 0$ and starts moving at $t = 0$.

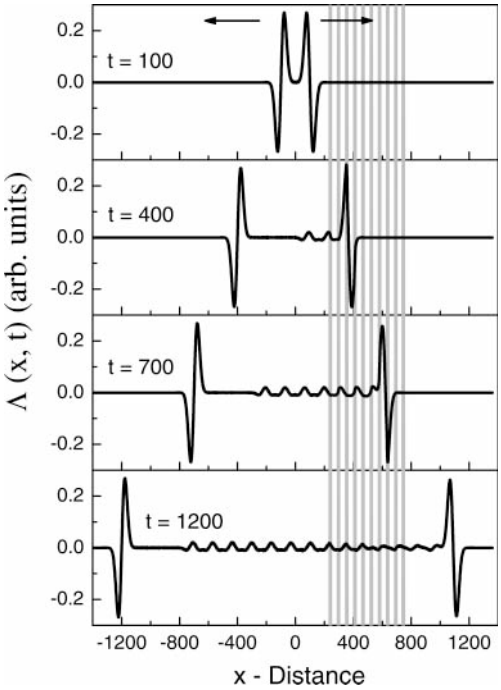

Fig. 7. Time evolution of a gaussian wavepacket put in front of an acoustic superlattice with ten periods. The pressure first derivative $\Lambda(x,t)$ is shown at different time steps. All the layers have the same acoustic impedance as the surrounding media. The initial wavepacket (not shown here) is put at $x_c = 0$ and starts moving at $t = 0$.

parameters $x_0 = 235$, $L = 10$, $d = 45$, and $N = 9$. The initial gaussian wavepacket, which is identical to the one used in the previous calculations, splits. Its components are shown at $t = 100$ in the upper panel in Fig. 5. The right component impinges on the superlattice, its shape changes slightly inside the superlattice, the peak maximum being practically constant. This property is a consequence of a constant acoustic ratio equal to 1; i.e. the system is transparent. At $t = 1200$, the packet moves freely out the far side of the superlattice. No appreciable numerical differences exist between the wave that has crossed the superlattice and the one that has moved freely in the opposite direction. Nevertheless, notice that some ripples appear in the plot. They represent the numerical inaccuracy of the method, but they can be suppressed by reducing the space step near the interfaces. In Fig. 6 the results for the other canonical variable, $\Lambda = \partial\Phi/\partial t$, are shown. The same analysis is valid for this entity.

Summary

We have presented a method that allows the simulations of sound propagation in the time domain for heterogeneous fluids in any dimension. The method is based on the split-operator technique, which is widely used in quantum mechanics. In comparison with standard finite-difference schemes, it has the following advantages: (i) it has a better accuracy in the time-domain, (ii) it works easier for large non-homogeneous space discretization, and (iii) it satisfies the energy conservation law. Here, we also have demonstrated its performance by solving several one-dimensional test problems.

Appendix: Glauber's formula for three non-commutative operators

It is known that if two operators A, B do not commute, the product of their corresponding single exponential operators is related with the exponential operator containing their sum in the exponent through the so called Glauber's formula:

$$\mathrm{e}^{-tA}\,\mathrm{e}^{-tB} = \mathrm{e}^{-t(A+B)}\,\mathrm{e}^{\frac{1}{2}t^2[A,B]}\,.$$

In what follows we extend this formula to the case of three distinct operators. Afterwards it will be applied to the case for which two of them are equal. It will be shown that the operator decomposition employed in Eq. (22) is of the order $(\Delta t)^3$; lower than the one obtained without the symmetric splitting of operator A (or B).

Let us consider the operator $F(\mathbf{r},t)$ described by:

$$F(\mathbf{r},t) = \mathrm{e}^{-tA}\,\mathrm{e}^{-tB}\,\mathrm{e}^{-tC}\,.$$

Its partial time derivative is:

$$\frac{\partial F(\mathbf{r},t)}{\partial t} = -\{A + \mathrm{e}^{-A}\,B\,\mathrm{e}^{tA} + \mathrm{e}^{-tA}\,\mathrm{e}^{-tB}\,C\,\mathrm{e}^{tB}\,\mathrm{e}^{tA}\} \times F(\mathbf{r},t)\,. \tag{67}$$

Operator properties allow one to write the operators B and C in the form:

$$B = \mathrm{e}^{tA}\,B\,\mathrm{e}^{-tA} - [\mathrm{e}^{tA},\,B]\,\mathrm{e}^{-tA}\,,$$
$$C = \mathrm{e}^{tA}\,\mathrm{e}^{tB}\,C\,\mathrm{e}^{-tB}\,\mathrm{e}^{-tA} - [\mathrm{e}^{tA}\,\mathrm{e}^{tB},\,C]\,\mathrm{e}^{-tB}\,\mathrm{e}^{-tA}\,.$$

Then, Eq. (67) becomes,

$$\frac{\partial F(\mathbf{r},t)}{\partial t} = -\{A + B + C + G(\mathbf{r},t)\}\,F(\mathbf{r},t)\,, \tag{68}$$

where

$$G(\mathbf{r},t) = [\mathrm{e}^{tA},\,B]\,\mathrm{e}^{-tA} + \left[\mathrm{e}^{tA}\,\mathrm{e}^{tB},\,C\right]\,\mathrm{e}^{-tB}\,\mathrm{e}^{-tA}\,.$$

We integrate Eq. (68) in the time interval $[0,\Delta t]$, where Δt is small compared with the temporal dependence of $A(\mathbf{r},t)$, $B(\mathbf{r},t)$ and $C(\mathbf{r},t)$, which are considered constant in the interval. Besides, if we assume that $F(\mathbf{r},t=0) = 1$, we obtain:

$$F(\mathbf{r},t) = \exp\left\{-\Delta t(A+B+C) + \int_0^{\Delta t} G(r,t)\,\mathrm{d}t\right\}.$$

Since

$$\mathrm{e}^{-\Delta t\,A} = \sum_{n=0}^{\infty}\frac{(-1)^n}{n!}\Delta t^n\,A^n\,,$$

we can cast the integral $\int_0^{\Delta t} G(\mathbf{r},t)\,\mathrm{d}t$ as an infinite sum of terms:

$$\int_0^{\Delta t} G(\mathbf{r},t)\,\mathrm{d}t = \sum_{n,m=0}^{\infty}\frac{\Delta t^{n+m+1}}{n!m!(n+m+1)}\,[A^n,B]\,A^m + \sum_{n,m,p,q=0}^{\infty}\frac{\Delta t^{n+m+p+q+1}}{n!m!p!q!(n+m+p+q+1)} \times [A^nB^m,\,C]\,B^pA^q\,.$$

Because Δt is small, we only need to consider a few terms of the infinite series,

$$\int_0^{\Delta t} G(\mathbf{r},t)\,\mathrm{d}t = \frac{\Delta t^2}{2}\{[A,B+C]+[B,C]\} + \frac{\Delta t^3}{6}\{[A^2,B+C]+[B^2,C]\} + \frac{\Delta t^3}{3}\{[AB,C]-[A,B]\,A-[(A+B),C] \times (A+B)\}+O[(\Delta t)^4].$$

If $A=C$, the terms of Δt^2 are cancelled and the last expression becomes

$$\int_0^{\Delta t} G(\mathbf{r},t)\,\mathrm{d}t = \frac{\Delta t^3}{6}\{[A^2,B]+[B^2,A] + 2[A,B]\,(A+B)\}+O[(\Delta t)^4]\,.$$

Then, the function $F(\mathbf{r},t)$, can be replaced by the identity

$$\mathrm{e}^{-\Delta t\,A}\,\mathrm{e}^{-\Delta t\,B}\,\mathrm{e}^{-\Delta t\,A} = \mathrm{e}^{-\Delta t(A+B+A)} \times \mathrm{e}^{-\frac{1}{6}\Delta t^3\{[A^2,B]+[B^2,A]+2[A,B](A+B)\}+O[(\Delta t)^4]}\,.$$

Notice that the combination of three operators in which two of them are equal produces the minimum error.

When $A=C=A/2$, we have the case of Eq. (22) and the error associated to the approximation involved in that equation can easily be calculate by taking the difference

$$Err = \mathrm{e}^{-\Delta t\frac{A}{2}}\,\mathrm{e}^{-\Delta t\,B}\,\mathrm{e}^{-\Delta t\frac{A}{2}} - \mathrm{e}^{\Delta t\left(\frac{A}{2}+B+\frac{A}{2}\right)-\frac{1}{24}\Delta t^3[(A+2B),[A,B]]}\,.$$

In conclusion,

$$Err = \frac{\Delta t^3}{24}\,[(A+2B),\,[A,B]]\,.$$

Acknowledgments. D. Bosquetti acknowledges a special grant provided by the Autonomous University of Madrid through its Office of International Relationships. J. Sánchez-Dehesa acknowledges useful discussions with P. Tarazona. The authors also wish to thank Prof. G. E. Marques, and Prof. E. Marega for their continuous support and interest in this work. The finantial support provide by the Spanish MEC (contract number TEC2004-03545/MIC) is also gratefully acknowledged.

References

[1] Sánchez-Pérez, J. V.; Caballero, D.; Martínez-Sala, R.; Rubio, C.; Sánchez-Dehesa, J.; Meseguer, J.; Llinares, J.; Gálvez, F.: Sound Attenuation by a Two-Dimensional Array of Rigid Cylinders. Phys. Rev. Lett. **80** (1998) 5325–5328.
[2] Cervera, F.; Sanchis, L.; Sánchez-Pérez, J. V.; Martínez-Sala, R.; Rubio, C.; Meseguer, F.; López, C.; Caballero, D.; Sánchez-Dehesa, J.: Refractive Acoustic Devices For Airborne Sound. Phys. Rev. Lett. **88** (2002) 023902.
[3] Caballero, D.; Sánchez-Dehesa, J.; Rubio, C.; Martínez-Sala, R.; Sanchez-Peérez, J. V.; Meseguer, F.; Llinares, J.: Larger two-dimensional sonic band gaps. Phys. Rev. E**60** (1999) R6316–6319.
[4] McLean, A. S.; Pendry, J. B.: A polarized transfer matrix for electromagnetic media. J. Mod. Opt. **41** (1994) 1781–1802.
[5] Sigalas, M. M.; Economou, E. N.: Attenuation of multiple scattered sound. Europhys. Lett. **36** (1996) 241–246.
[6] Sanchis, L.; Cervera, F.; Sánchez-Dehesa, J.; Sánchez-Pérez, J. V.; Rubio, C.; Martínez-Sala, R.: Reflectance properties of two-dimensional sonic band-gap crystals. J. Acoust. Soc. Am. **109** (2001) 2598–2602.
[7] Chen, Y. Y.; Yee, Z.: Acoustic Attenuation by Two-dimensional Arrays of Rigid Cylinders. Phys. Rev. Lett. **87** (2001) 184301.
[8] Sanchis, L.; Hakansson, A.; Cervera, F.; Sánchez-Dehesa, J.: Reflectance properties of two-dimensional sonic band-gap crystals. Phys. Rev. B**67** (2003) 035422.
[9] Psarobas, I. E.; Stefanou N.; Modinos, A.: Scattering of elastic waves by periodic arrays of spherical bodies. Phys. Rev. B**62** (2000) 278–291.
[10] Yee, K. S.: Numerical Solution of initial boundary value problems involving Maxwell equations in isotropic media. IEEE trans. Antennas Propagat. **AP-14** (1966) 302–307.
[11] Wang, S.: Finite-difference time-domain approach to underwater acoustic scattering problems. J. Acoust. Soc. Am. **99** (1996) 1924–1928.
[12] Stephen, R. A.: A review of finite-difference method for seismo-acoustic problems at seafloor. Rev. Geophys. **26** (1988) 445–458.
[13] Sigalas, M. M.; García, N.: Importance of coupling between longitudinal and transverse components for the creation of acoustic band gaps: The aluminum in mercury case. Appl. Phys. Lett. **76** (2000) 2307–2309; Theoretical study of three dimensional elastic band gaps with the finite-difference time-domain method. J. Appl. Phys. **87** (2000) 3122–3125.
[14] Feit, M. D.; Fleck, J. A.; Steiger, A.: Solution of the Schrödinger Equation by a Spectral Method. J. Comp. Phys. **47** (1982) 412–433.
[15] Bosquetti, D.; Sánchez-Dehesa, J.: The split-operator technique in acoustical physics, in Diffraction and Scattering in Fluid Mechanics and Elasticity. (Abrahams, D.; Martin, P. A.; Simon, M. J., eds.). Kluwer Academic Publishers, (2002) 107–114.
[16] Cohen-Tannoudji, C.; Diu, B.; Laloë, F.: Mecanique Quantique. John Wiley and Sons Inc, 1977.
[17] Dattoli, G.; Ottaviani, P. L.; Segreto, A.; Torre, A.: Symmetric-split-operator techniques and finite difference methods for the solution of classical and quantum evolution problems. Il nuovo Cimento **111** (1996) 825–839.
[18] Goldstein, H.: Classical Mechanics. Addison Wesley, 1980.
[19] Dowling, J. P.: Sonic band structure in fluids with periodic density variations. J. Acoust. Soc. Am. **91** (1992) 2539.
[20] Towne, D. H.: Wave phenomena. Dover, New York, 1966.